

Tailoring the Charge Carrier Lifetime Distribution of 10 kV SiC PiN Diodes by Physical Simulations

Zimo Yuan^{1,a*}, Adolf Schöner^{2,b}, Sergey Reshanov^{2,c}, Wlodek Kaplan^{2,d},
Mietek Bakowski^{3,e} and Anders Hallén^{1,f}

¹KTH Royal Institute of Technology, EECS, Isafjordsgatan 22, SE-164 40 Kista, Sweden

²II-VI Kista AB, SE-164 40 Kista, Sweden

³RISE Acreo Swedish ICT AB, Box 1070, SE-164 25 Kista, Sweden

^azimo@kth.se, ^badolf.schoner@II-VI.com, ^csergey.reshanov@II-VI.com,

^dwlodek.kaplan@II-VI.com, ^emietek.bakowski@ri.se, ^fahallen@kth.se

Keywords: Proton Implantation, Shockley-Read-Hall (SRH) Lifetime, IV characteristics, reverse recovery.

Abstract. In this paper, Shockley-Read-Hall (SRH) lifetime depth profiles in the drift layer of 10 kV SiC PiN diodes are calculated after MeV proton implantation. It is assumed that the carbon vacancy is the domination trap for charge carrier recombination and the SRH lifetime is calculated with defect parameters from the literature and proton-induced defect distributions deduced from SRIM calculations. The lifetime profiles are imported to Sentaurus TCAD and static and dynamic simulations using tailored lifetime profiles are carried out to study the electrical effect of proton implantation parameters. The results are compared to measurements, specializing on optimization of the trade off between on-state and turn-off losses, represented by the forward voltage drop, V_T , and reverse recovery charge, Q_{rr} , respectively. Both the simulated and measured IV characteristics show that increasing proton dose, or energy, has the effect on increasing forward voltage drop and on-state losses, while simultaneously, the localized SRH lifetime drop decreases the plasma level, increases the speed of recombination and decreases reverse recovery charge. Finally, TCAD simulations with different combinations of proton energies and fluences are used to optimize the trade-off between static and dynamic performances. Reverse recovery charge and forward voltage drops of these groups of diodes are plotted together, showing that a medium energy which induces the most defects in the depletion region relatively close to the anode gives the best dynamic performances, with a minimum degradation of static performance.

Introduction

Reaching an optimal balance between static and dynamic performances is essential for most power devices, for instance bipolar 4H-SiC devices, such as PiN diodes, especially in circuits where high switching frequencies are required. MeV low mass ion implantation is an off-line technique that allows for tailoring this trade-off after device fabrication and enables optimized design for different application frequencies.

The switching losses of PiN diodes are dependent on total amount of stored charge and the speed to remove them by recombination, both of which are related to Shockley-Read-Hall (SRH) lifetime in the low-doped drift region. High-energy proton implantation, which was first demonstrated for Si thyristors [1] and applied to silicon PiN diodes [2], has a strong penetrating ability and can introduce defects that reduce SRH lifetime locally without causing too much damage to the entire device. The extra defects introduced by elastic collisions with Si and C lattice atoms form point defects with deep levels in the bandgap and decrease carrier concentrations. The localized deep level traps shorten the turn-off time, but also increase the resistivity, leading to an increased forward voltage drop. Today it is well established that the carbon vacancy, V_C , is the most dominant lifetime killing defect after energetic particle irradiation in 4H-SiC [3, 4]. The depth distribution of this defect, $N_T(x)$, and the parameters controlling the carrier lifetimes, i.e. bandgap position, E_T , and capture cross sections for

electrons and holes, $\sigma_{n/p}$, can be obtained from measurements, such as deep level transient spectroscopy (DLTS). Thus, it is possible to calculate SRH lifetime profiles of different combinations of implantation energies and fluences, whereafter these profiles can be used for device simulations aiming for an optimized balance between on-state and switching losses in a specific circuit application.

In this paper, static and dynamic simulations of 10 kV 4H-SiC diodes using Sentaurus TCAD are combined with calculation of lifetime profiles estimated by SRIM [5] and DLTS data from the literature. The calculated lifetime depth profiles are imported to Sentaurus TCAD for static and dynamic simulations. Measured static IV characteristics of diodes irradiated with different proton energies and doses are used to calibrate the simulation results. A shift to the right of IV characteristics is observed both for increasing energies and doses. Dynamic performances of these diodes are evaluated by reverse recovery simulations. Increasing doses has a positive effect on decreasing the peak reverse current and reverse recovery charge (Q_{rr}). Finally, the trade-off between static and dynamic performances of diodes are optimized and discussed.

About the Experiment and Simulations

The 10 kV SiC PiN diodes, with an active anode area of $7.9 \times 10^{-3} \text{ cm}^2$, are first characterized in Ref. [6]. Table 1 shows implantation parameters of three different groups of diodes, each group contained 4 diodes and mean value of the group was used. For the implantation, an extra 30 μm thick Al absorbing foil was used for 1.9 MeV irradiations to reduce the energy, so the damage peak appears close to the anode junction. This is needed since the 5 MeV tandem accelerator used for the proton implantation is not stable below 1 MeV.

In this paper, the carbon vacancy is considered as the dominant lifetime controlling defect. Total carbon vacancy densities under different implantation energies and fluences are simulated with SRIM [5], but only 4% of which will contribute to effective defect density due to dynamic annealing [7]. A concentration of $2.7 \times 10^{12} \text{ cm}^{-3}$ of intrinsic carbon vacancies is added to the SRIM results to set the defect concentration $N_T(x)$ in the non-implanted region of the drift layer. This value is tuned to produce experimental values of forward voltages comparable to the measured data [6, 8].

The carbon vacancy-induced SRH lifetime is calculated as:

$$\tau^{-1} = \frac{(\Delta n + n_0)c_n c_p N_T(x)}{c_n(n_0 + \Delta n + n_1) + c_p(p_0 + \Delta p + p_1)}. \quad (1)$$

where n_0 and p_0 are equilibrium concentrations of electrons and holes while Δn and Δp are injected excess carrier concentrations, n_1 and p_1 are carrier concentrations when the Fermi level is in agreement with the bandgap level of the trap, and for the carbon vacancy, these are small enough to be neglected at room temperature. Capture coefficients of electrons and holes $c_{n/p}$ are calculated using thermal velocities $v_{n/p}$ and capture cross sections $\sigma_{n/p}$ from literature, as deduced from DLTS measurements. It should be noted that, for the carbon vacancy, these cross sections are normally measured around room temperature, but cannot be used for other temperatures since the vibration entropy factor involved in the recombination process cannot be independently determined. The used parameters are shown in Table 2 [4, 9]. Equation 1 will result in a lifetime equal to the minority carrier lifetime for low injection level and the sum of minority and majority carrier lifetimes for the high injection level. In this work Auger recombination is not considered and no temperature dependence is included in this paper. The calculated hole profiles of three groups of diodes are shown in Fig. 1.

Table 1. Energies and doses of protons for different groups of experimental diodes.

Group	Energy [MeV]	Dose [cm^{-2}]
A	1.9 (including Al foil)	5×10^{10}
B	3.4	2×10^{10}
C	3.4	5×10^{10}

Table 2. Carbon vacancy parameters used to calculate SRH lifetime in Matlab.

Bandgap position [eV] [4]	0.7
Electron capture cross section in n- epilayers [cm^2] [9]	2×10^{-14}
Hole capture cross section in n- epilayers [cm^2] [9]	3.5×10^{-14}

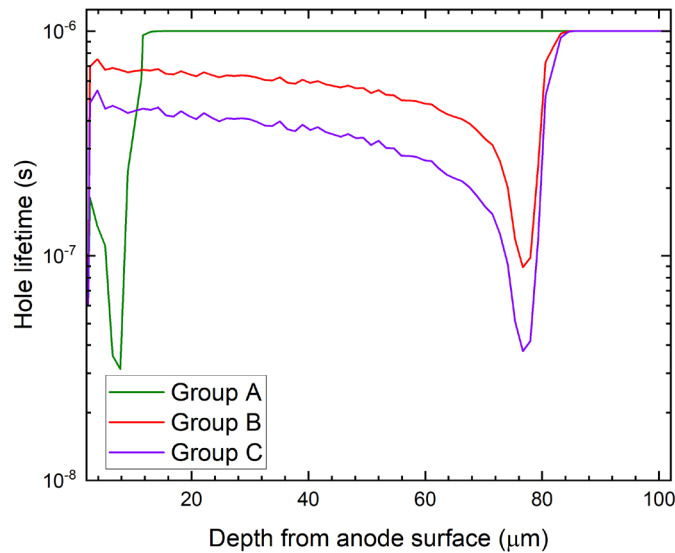


Fig. 1. Calculated hole lifetime profiles of three groups of diodes with Matlab.

Results and Analysis

Room temperature is used in all the simulations. One diode simulation with constant electron and hole lifetime in the drift region, calculated only with intrinsic concentration of carbon vacancies, is used as a reference group. The forward voltages at specific current densities from simulated IV characteristics of these four groups (A, B, C and reference) are plotted together with measurement results in Fig. 2. Forward voltage values increase with implantation energies and fluences since the resistivity of the drift region increases more when more carriers are recombined due to the defects. A discrepancy between simulated and measured results is observed especially for group C (dashed line). This can be due to external resistance not included in the simulations (contact resistance, oxide resistance, etc.) or difficulties with the measurements [10, 11].

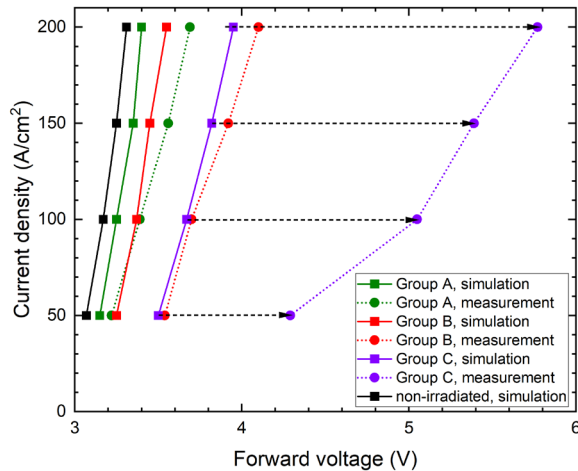


Fig. 2. Increasing proton energies or doses cause increase in forward voltages. Discrepancy between simulations and measurements comes probably from a resistive load.

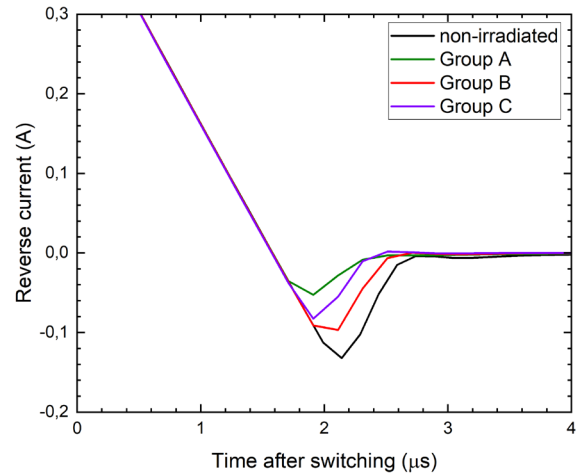


Fig. 3. Simulated reverse recovery behaviors from a pulse circuit. The lower implantation energy corresponds to a smaller Q_{rr} .

Sentaurus TCAD allows device/circuit mixed-mode simulations. A simplified double pulse circuit from Ref. [12] was used for the reverse recovery simulations. Parameters of elements in the circuit, for instance DC voltage source and inductors, are adjusted to get a similar on-state injection level and di/dt as the measurements in Ref. [13]. The simulated reverse recovery currents versus time are shown in Fig. 3. The area covered by reverse current curve, also known as Q_{rr} , is a key parameter for calculating turn-off losses in bipolar devices and for evaluating dynamic performances. The Q_{rr} of group C is clearly smaller than that of group B, showing that higher dose of protons decreases Q_{rr} more by reducing the charged carriers stored in drift region. Group A, however, shows a smaller Q_{rr} compared to group C with a much higher energy.

Proton implantation effects can also be examined by simulating the charge carrier plasma distribution as a function of turn-off time. Figure 4 shows simulated time-variant hole concentrations of group A and C. Higher energy protons create defects in a larger area, which contribute to a lower average hole concentration and thus cause a higher increase in resistivity and forward voltage drop, as seen for group C. However, the lower energy group, A, affects more carriers inside the depletion region close to the anode (highlighted with red circle), which dominate the reverse recovery current. It can also be seen that within 2 μs after switching, holes close to the pn junction of group A recombine faster than group C. A similar faster decrease of the hole plasma also happens close to the buffer layer for group C, which has a lower lifetime than group A in this region.

To tailor and optimize the trade-off between static and dynamic performances, more simulations with various implantation energies and fluences are carried out. Reverse recovery charge, normalized to the simulated value with constant lifetimes, and forward voltage drop at a current density of 200 A/cm², representing switching losses and on-state losses, respectively, are plotted in Fig. 5. For each energy, increasing fluences of 2×10^{10} , 5×10^{10} , 1×10^{11} and 2×10^{11} cm⁻², giving decreasing lifetime, are used in the simulations. By increasing the dose for the same energy, the trade-off curve moves downwards and to the right, but different energies will show different curves. Low-energy irradiations with Al absorbing foil give smallest increase in forward voltage, but weaker decrease in Q_{rr} at low doses compared to other groups, probably since the relatively high plasma level close to the anode makes it less sensitive to lifetime variation. The trade-off, however, can be improved by simply using higher doses. The best trade-off among all the simulated parameters is reached when the lifetime killing peak is very close to the anode with a dose over 1×10^{11} cm⁻². Figure 5 also shows the possibility to minimize total losses for bipolar devices especially used in fast-switching applications by tailoring lifetime profiles.

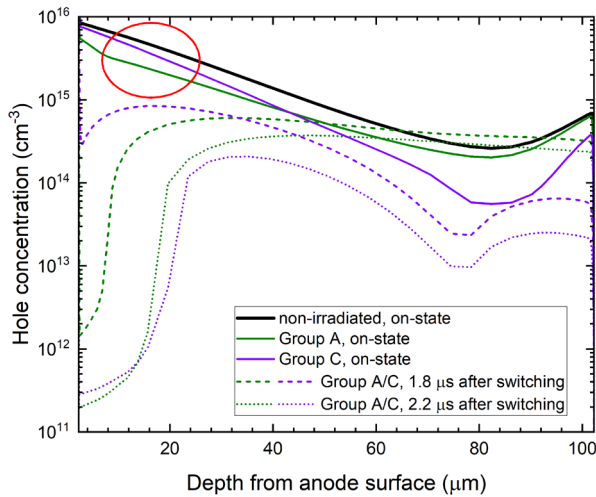


Fig. 4. Simulated hole plasma levels before and after switching. The plasma level and speed of plasma reduction are both related to proton-induced defects location.

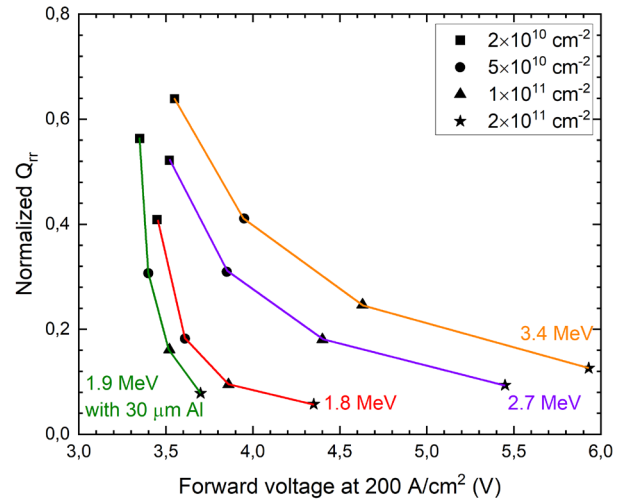


Fig. 5. Optimized trade-off between on-state and switching losses. 1.9 MeV protons absorbed by Al foil give the best dynamic performance without causing too much increase in forward voltage.

Summary

The SRH lifetime profiles calculated in Matlab are imported into Sentaurus TCAD model of a 10 kV 4H-SiC PiN diode. The simulations are compared to real devices that has been measured after proton implantation to reduce the charge carrier lifetime locally in the drift layer. Higher proton doses increase forward voltage and decrease Q_{rr} , which is also true for higher energies, placing the damage peak deeper in the drift region. The simulations also show that a 1.9 MeV proton implantation with a 30 μm thick Al absorbing foil, reaching a depth of about 10 μm , with a dose higher than $1 \times 10^{11} \text{ cm}^{-2}$ makes it possible to obtain a Q_{rr} which is less than 10% of non-irradiated diodes, while the increase of forward voltage drop at 200 A/cm^2 is only around 0.6 V. This optimization process can be merged into the design process before fabrication and is useful when lower switching losses are required for the devices. The proton implantation technique also makes it possible to optimize the charge carrier lifetime profile in devices for different operating frequencies and obtain minimal combination of turn-off and steady state losses.

Acknowledgement

We appreciate support from the Ion Technology Centre, ITC, at Uppsala University, Sweden, for MeV proton implantations.

References

- [1] V.A.K. Temple, F.W. Holroyd, IEEE Trans. Electron Devices, ED-30, 7, 782 (1983)
- [2] R. Brammer, A. Hallén, and J. Håkansson, "Simulation of Proton-Induced Local Lifetime Reduction in 10 kV Diodes", IEEE Trans. Electron Devices 40, 2089, (1993)
- [3] Son, Nguyen Tien, et al. "Negative-U system of carbon vacancy in 4H-SiC." Physical review letters 109.18 (2012): 187603.
- [4] Hazdra, Pavel, and Stanislav Popelka. "Lifetime control in SiC PiN diodes using radiation defects." *Materials Science Forum*. Vol. 897. Trans Tech Publications Ltd, 2017.
- [5] Stopping and range of ions in matter SRIM-2013, downloadable from <http://www.srim.org/>

- [6] M. Bakowski *et al.*, "Design and Characterization of Newly Developed 10 kV 2 A SiC p-i-n Diode for Soft-Switching Industrial Power Supply," *IEEE Transactions on Electron Devices*, vol. 62, no. 2, pp. 366–373, 2015, doi: 10.1109/TED.2014.2361165.
- [7] Ayedh, H. M., et al. "Formation of carbon vacancy in 4H silicon carbide during high-temperature processing." *Journal of Applied Physics* 115.1 (2014): 012005.
- [8] Salemi, Arash, et al. "Conductivity modulated on-axis 4H-SiC 10+ kV PiN diodes." *2015 IEEE 27th International Symposium on Power Semiconductor Devices & IC's (ISPSD)*. IEEE, 2015
- [9] Klein, P. B., et al. "Lifetime-limiting defects in n- 4H-SiC epilayers." *Applied Physics Letters* 88.5 (2006): 052110.
- [10] Bryant, A. T., et al. "Physical modelling of large area 4H-SiC PiN diodes." *2009 IEEE Energy Conversion Congress and Exposition*. IEEE, 2009.
- [11] Jacobs, Keijo, et al. "Static and Dynamic Performance of Charge-Carrier-Lifetime-Tailored High-Voltage SiC PiN Diodes with Capacitively Assisted Switching." *IEEE Transactions on Power Electronics* (2022).
- [12] Lutz, Josef, et al. "Semiconductor power devices." *Physics, characteristics, reliability* 2 (2011), pp. 233-236.
- [13] Yuan, Zimo, et al. "Localized Lifetime Control of 10 kV 4H-SiC PiN Diodes by MeV Proton Implantation." *Materials Science Forum*. Vol. 1062. Trans Tech Publications Ltd, 2022.